Am J Transl Res 2021;13(1):301-313
www.ajtr.org /ISSN:1943-8141/AJTR0105951

Original Article

IFN-α facilitates the effect of sorafenib via shifting the M2-like polarization of TAM in hepatocellular carcinoma

Ze Zhang[1*], Ying Zhu[1*], Da Xu[1*], Tian-En Li[1], Jian-Hua Li[1], Zi-Tian Xiao[1], Mo Chen[1], Xin Yang[1], Hu-Liang Jia[1,2], Qiong-Zhu Dong[1,2,3], Lun-Xiu Qin[1,2,3]

[1]Department of General Surgery, Huashan Hospital of Fudan University, Shanghai 200040, China; [2]Cancer Metastasis Institute, Huashan Hospital of Fudan University, Shanghai 200040, China; [3]Institutes of Biomedical Sciences, Fudan University, Shanghai 200040, China. [*]Co-first authors.

Received December 5, 2019; Accepted November 20, 2020; Epub January 15, 2021; Published January 30, 2021

Abstract: Tumor-associated macrophages (TAMs) and how they are activated play critical roles in tumor progression and metastasis, and in hepatocellular carcinoma (HCC), they are associated with sorafenib resistance. Reprogramming of TAMs into M1-like macrophages has been proposed as an approach to stimulate tumor regression. Here we studied the collective effects of interferon-alpha (IFN-α) and sorafenib on HCC. We found that IFN-α delayed tumor growth and inhibited pulmonary metastasis in an orthotopic HCC implantation model. Via *in vitro* studies, we found that IFN-α treatment could reprogram M2-like RAW264.7 and THP-1 macrophage cells toward M1-like cells. In addition, we also found that IFN-α combined with a low dose of sorafenib has a synergistic inhibitory effect on HCC tumor growth and pulmonary metastasis without obvious toxicity in an *in vivo* mice model. Moreover, IFN-α increased sorafenib's therapeutic efficacy by shifting TAM polarization to an M1-like phenotype, increasing and activating intratumoral $CD8^+$ T cells in HCCs. In conclusion, a combination of IFN-α and sorafenib have synergistic inhibitory effects on HCC growth and metastasis resulting from a shift in TAM polarization rather than their depletion. Our study supports the future clinical use of a combination of IFN-α and sorafenib for the treatment of advanced HCC.

Keywords: Tumor-associated macrophages, interferon-alpha, immunotherapy, tumor microenvironment, sorafenib

Introduction

Hepatocellular carcinoma (HCC) is one of the most lethal malignancies globally, and many HCC patients have reached advanced stages at the time of their diagnosis and are, therefore, not suitable for curative treatments [1, 2]. Currently, sorafenib has been established as a first-line therapy for advanced HCC. Sorafenib is a multi-kinase inhibitor that affects a number of protein kinases, including VEGFR, PDGFR, and RAF, and it can promote cell apoptosis, reduce angiogenesis and inhibit tumor proliferation [3]. However, it has only a limited effect on overall survival (OS) and exhibits a poor response rate [4]. Therefore, new strategies are urgently needed to improve the effectiveness of targeted HCC therapies.

Immunotherapy is now hailed as a major advance in cancer treatment. In some cancer patients, immune checkpoint blockade, CAR-T therapy, and cytokine therapy treatment, have been shown to have robust benefits [5-9]. Unfortunately, only a small fraction of HCC patients benefit from these therapeutic approaches, and the low response to immunotherapy is partly due to the formation of immunosuppressive tumor microenvironments and T-cell exhaustion [10]. Infiltration by multiple types of immune cells, including TAMs, promotes the development of immunosuppressive microenvironments that can support the initiation and progression of HCC [11].

Macrophages are extremely versatile, multifunctional cells. Currently, two macrophage subtypes have been identified, i.e., classically activated macrophages (M1) and alternatively activated macrophages (M2) [11]. Inhibition of inflammatory cytokine secretion by HCC cells can "educate" recruited peripheral blood monocytes such that they differentiate into macrophages exhibiting an M2-like phenotype.

Recently, accumulating evidence has revealed that TAMs can modulate tumor immune microenvironments and promote HCC progression; for example, the polarization of TAMs into the M1 phenotype can limit tumor growth and extend survival in tumor-bearing mice [12, 13], and TAM depletion can enhance sorafenib's antitumor effect in HCC models [14].

IFN-α has been widely used to treat malignancies, including HCC [15-17]. Multiple clinical trials have revealed that adjuvant IFN-α therapy can increase survival in HCC patients following curative resection [18]. The limited clinical application of IFN-α is mainly due to the inability to identify patients who will respond effectively [18, 19]. The anti-tumor effect of IFN-α is due to its indirect inhibitory effects on tumor cells, including its immunomodulatory effects [20]. The immune-modulatory effects of IFN-α include the regulation of macrophage polarization and immune cell infiltration [21]. Recently, IFN-β was demonstrated to dramatically enhance the antitumor effect of anti-EGFR Ab [22].

Here we found that IFN-α has a synergistic effect with sorafenib on inhibiting HCC growth and metastasis. Further investigation revealed that this synergistic effect might result from TAM polarization toward the M1-like phenotype and attenuation of the immune suppressive microenvironment. These findings support the potential clinical use of sorafenib in combination with IFN-α for HCC treatment.

Materials and methods

Cell lines and animal models

Mouse Hepa1-6 HCC cells, human Huh7 HCC cells, and murine monocyte/macrophage RAW264.7 cells were cultured in Dulbecco's modified Eagle's medium (DMEM) with 10% fetal bovine serum (FBS). Human THP-1 monocytes were cultured in 1640 with 10% FBS. All cell lines were provided by the Shanghai Institute of Cell Biology (Chinese Academy of Sciences, Shanghai, China).

Six-week-old male C57BL/6 mice were purchased from the SLAC Laboratory Animal Company (Shanghai, China). All animal experiments were approved by the Ethics Committee of Fudan University. The subcutaneous tumor model is established via subcutaneous implantation of 1×10^6 Hepa1-6 cells into the flanks of mice. Mice bearing tumors of approximately 50 mm^3 in volume were randomly partitioned into 4 groups (n = 6 mice/group): (a) oral use of vehicle and intratumoral injection of PBS (vehicle group); (b) oral use of sorafenib (30 mg/kg/day) (sorafenib group); (c) intratumoral injection of IFN-α (1.5×10^7 U/kg/day) (IFN-α group); (d) oral use of sorafenib (30 mg/kg/day) in combination with intratumoral injection of IFN-α (1.5×10^7 U/kg/day) (sorafenib and IFN-α combination group).

To generate the orthotopic model, subcutaneous tumors were harvested and dissected into pieces of approximately 1 mm^3, which were then orthotopically implanted into the liver parcel of other mice. 14 days after orthotopic implantation, the mice were randomly partitioned into 4 groups (n = 5 for each group) that received the same treatments used in the subcutaneous HCC model.

Flow cytometry analysis (FACS)

Single cell suspensions were prepared from fresh mouse tumors by using the mouse tumor dissociation kit following the manufacturer's instructions (Miltenyi Biotec). After red blood cell lysis, the cells were centrifuged for 5 minutes at 500×g before being suspended in FACS buffer. To avoid non-specific binding, cells were incubated with anti-mouse CD16/32 antibody for 15 minutes. The cells were then incubated with primary antibody at room temperature (RT) for 30 minutes in the dark, washed twice in phosphate-buffered saline (PBS), suspended in 300 μl of PBS, and then analyzed with a FACS Aria II instrument (BD Biosciences, San Jose, CA). The following antibodies from Biolegend (San Diego, California, USA) were used for cell staining to detect tumor-infiltrated immune cells: FITC-CD11b, PE-CD206, APC-CD4, PE-cy7-CD8, and APC-F4/80.

Quantitative real-time polymerase chain reaction (qPCR)

Trizol (Invitrogen, California, USA) was used for extraction of total RNA from cells and frozen samples. The RNA was then reverse transcribed into cDNA. Real-time PCR was performed with SYBR Green PCR Master Mix (DBI Bioscience, Denmark) in an ABI PRISM 7900

Sequence Detection System (Applied Biosystems). To quantify the mRNA levels, the measurements were normalized to GAPDH. The primer sequences used in this study are provided in Supplementary Table 1.

Enzyme-linked immune-sorbent assay (ELISA)

The culture supernatant of the cells to be examined was collected and centrifuged to remove interfering particles. ELISA kits were used to detect the IL-1b, IL-10, TGF-β1, IFN-γ and TNF-α levels following the manufacturer's instructions (R&D Systems, Minneapolis, Minnesota, USA).

M2-like macrophage polarization of RAW264.7 and THP-1

20 ng/ml IL-13 (Invitrogen Inc., Carlsbad, CA, USA) was used to stimulate RAW264.7 and THP-1 macrophages to polarize into the M2 phenotype, and the levels of the murine M2 macrophage marker CD206, the human M2 macrophages marker CD163, and the human M1 macrophage marker HLA-DR were detected via flow cytometry. Next, cytokines were detected via ELISA and the expression levels of macrophage polarization-related genes were measured via qPCR.

Cell counting Kit-8 (CCK-8)

5×10 cells/well were seeded in 96-well plates. After culturing to a specific time point, the numbers of viable cells were determined via the Cell Counting Kit-8 (CCK-8) (Dojindo Molecular Technology, USA). The optical density (OD) of the medium at a wavelength of 450 nm was measured with a spectrophotometer.

Colony formation assay

1000 cells per well were inoculated in 6-well plates. Next, approximately 2 ml of culture medium was added to each well, and even distribution of the cells was confirmed. The medium was changed once a week, being careful not to disturb the cells. After approximately 4 weeks, the medium was discarded, and the cells were washed thrice in PBS, fixed with 4% paraformaldehyde for 15 minutes, and then washed thrice in PBS. The cells were then stained with crystal violet (0.5%) for 10 minutes at RT, followed by rinsing with distilled water. After drying at RT, the cell clones were counted.

Migration and invasion assay

The ability of the HCC cells to migrate and invade was assessed in transwell chambers with 8-μm pore size polycarbonate membranes between the upper and lower chambers (BD Pharmingen). The bottom chamber contained DMEM with 10% FBS, which acts as a chemoattractant. 5×10^4 cells (for migration, without prepared matrigel) and 10×10^4 cells (for invasion, with prepared matrigel) were suspended in serum-free medium and seeded into the upper chambers. The assay plates were incubated at 37°C in a humidified incubator maintained with 5% CO_2.

Statistical analyses

SPSS 16.0 for Windows (IBM, Armonk, NY) was used for the statistical analyses. Between-group differences were analyzed via an unpaired two-tailed Student's *t* test or one-way ANOVA. The chi-square test or Fisher's exact test were used to analyze categorical data. Survival curves were calculated via the Kaplan-Meier method and compared via the log-rank test. *P* values less than 0.05 indicated statistically significant differences.

Results

IFN-α enhances the anti-tumor effect of sorafenib on HCC

We established subcutaneous implantation models in C57BL/6 mice with Hepa1-6 cells, which we then treated with IFN-α, sorafenib, or a combination of both. We found that sorafenib alone could inhibit HCC tumor growth, but that a much more robust inhibition was obtained when sorafenib was used in combination with IFN-α (**Figure 1A-D** and Supplementary Figure 1A).

To further evaluate the effects of these treatments on HCC growth and metastasis, we established orthotopic implantation models based on the above Hepa1-6 model (**Figure 1E**). Consistently, we observed that administration of sorafenib alone could inhibit tumor growth and lung metastasis (**Figure 1E-G**), but that a combination induced more robust decreases in tumor size and lung metastasis (**Figure 1I**) and increased the survival time ($P < 0.01$; **Figure 1H**) in the tumor-bearing mice compared with the effects of sorafenib or IFN-α

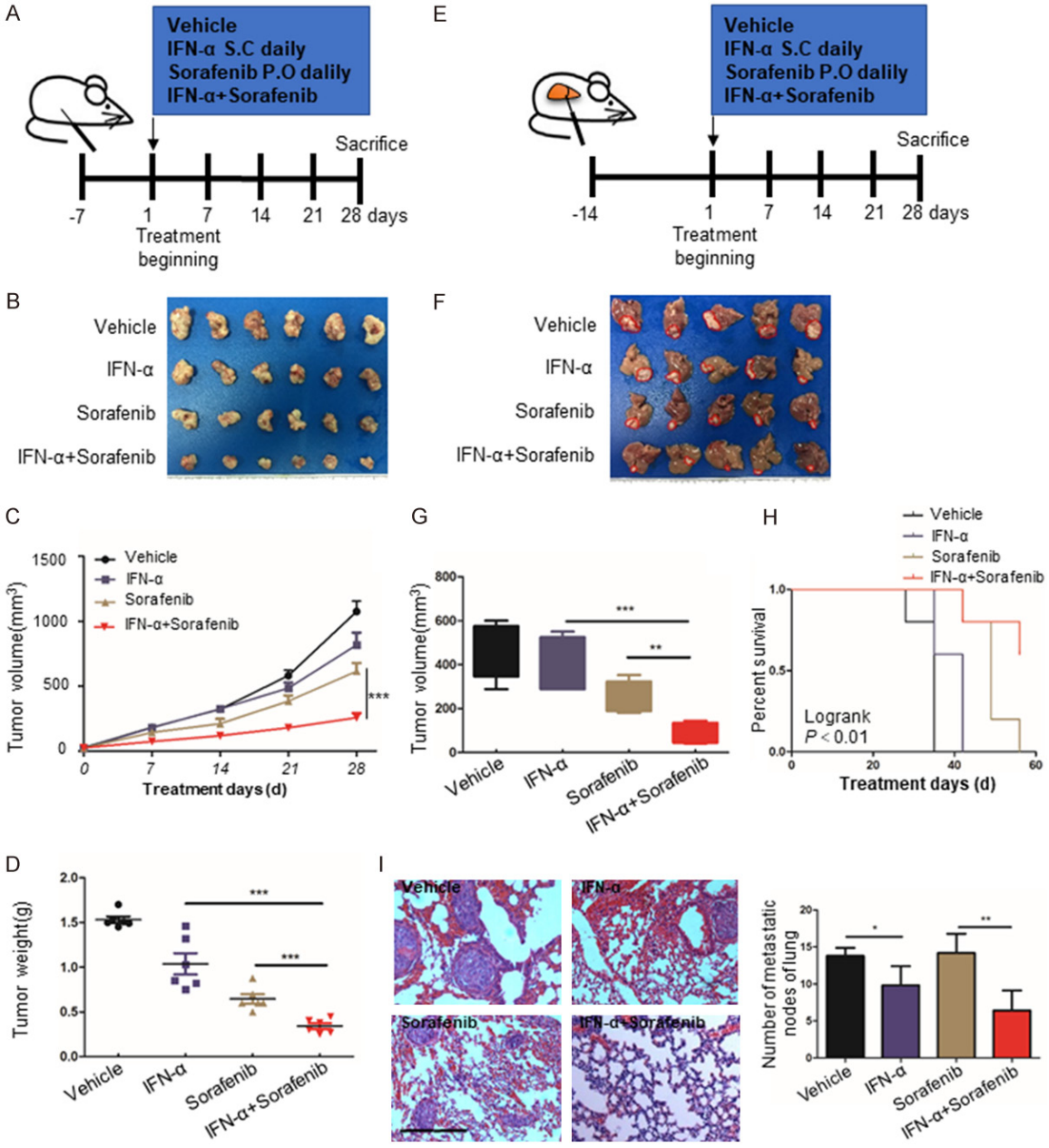

Figure 1. IFN-α enhances the anti-tumor effects of sorafenib. (A) Schematic description of IFN-α and sorafenib treatment in the subcutaneous tumor model. (B-D) Representative micrographs of the subcutaneous liver cancer model after treatment with vehicle, IFN-α, sorafenib, or the combination. Tumor growth was measured as (C) the tumor volume at different time points. (D) Tumor weight at the time of sacrifice. (E) Schematic description of IFN-α and sorafenib treatment in the orthotopic liver cancer model. (F, G) Representative micrographs of orthotopic liver tumors after treatment with vehicle, IFN-α, sorafenib, or the combination. (G) Tumor volume at the time of sacrifice. (H) Survival of mice bearing orthotopic Hepa1-6 tumors following IFN-α and sorafenib treatment. Significance was determined via the log rank test. (I) Left, representative images of Hematoxylin and Eosin (HE)-stained lung sections in the treatment groups. Scale bar, 200 μm. Right, the numbers of lung metastatic foci for each group. Error bars indicate mean ± SEM. $*P < 0.05$, $**P < 0.01$ and $***P < 0.001$. IFN-α, interferon-alpha; P.O., per os; S.C., subcutaneous injection.

alone. Moreover, we did not observe any appreciable differences in treatment toxicity (as indicated by body weight) among the different treatment groups (Supplementary Figure 1B). These results suggested that IFN-α dramatically enhanced sorafenib's antitumor effect on

HCC and that it had synergetic effects with sorafenib on HCC growth and metastasis. The combined treatment was more effective in combating HCC.

IFN-α inhibits macrophage activation and M2-like polarization in tumor microenvironments

To explore the underlying mechanism, we performed flow cytometry analysis (FACS) using F4/80, CD11b and CD206, and immunohistochemical (IHC) staining to detect intratumoral macrophages in orthotopic implantation models. We found that IFN-α treatment reduced the number of infiltrated M2-like macrophages ($F4/80^+CD206^+$ cells and $F4/80^+CD11b^+$ cells) (**Figure 2A**, **2B**) and increased the number of M1-like macrophages (iNOS) in Hepa1-6 tumors (**Figure 2C**). These results indicated that IFN-α treatment induced a shift in TAM polarization from an M2- to an M1-like phenotype in HCC.

To explore the effect of IFN-α on macrophage polarization, we used IL-13 to induce M2-like polarization and then treated the polarized cells with IFN-α. As shown in **Figure 3A**, we observed a significant upregulation of CD206 in RAW264.7 murine macrophages treated with 20 ng/ml of IL-13 for 72 h that was robustly reduced after IFN-α treatment (10^4 U/mL). Via qPCR, we found that the mRNA levels of M2 markers, i.e., Arg1 and IL-10, were significantly downregulated, while those M1 markers, i.e., iNOS, IL-1b, and TNFα, were upregulated after IFN-α treatment (**Figure 3B**). ELISAs demonstrated a reduction in the IL-10 protein level (an M2 marker) in the supernatant of IFN-α-treated macrophages, while the IL-1b level (an M1 marker) was clearly elevated (**Figure 3C**). In addition to its effect in murine macrophages, IFN-α treatment also significantly inhibited the M2-like shift of phorbol-12-myristate-13-acetate (PMA)-treated human THP-1 cells induced by IL-13 (**Figure 3D-F**). These results provided further evidence supporting the notion that IFN-α treatment can effectively inhibit M2-like macrophage polarization, thus inducing a shift of TAMs from an M2- to an M1-like phenotype in the tumor microenvironment.

IFN-α neutralizes the promoting effects of M2-like macrophages on HCC cell proliferation and invasion

M2-like macrophages have been previously shown to promote the progression and metastasis of HCC; therefore, we further explored the effects of IFN-α on the functional roles of macrophages in HCC cell behaviors. Murine (RAW264.7) and human (PMA-treated THP-1) macrophages were treated for 72 h with IL-13, IFN-α, or a combination. The culture medium (CM) was then replaced with fresh medium without serum, and the supernatant was collected 24 h later. The CM from IL-13-treated macrophages significantly enhanced cell viability (**Figure 4A** and **4D**), as well as the colony formation (**Figure 4B** and **4E**), migration, and invasion (**Figure 4C** and **4F**) abilities of HCC cells (Hepa1-6 and Huh7). By contrast, the CM from the IL-13 and IFN-α combination group did not have any significant promoting effects on HCC cells. These results indicated that IFN-α could neutralize the promoting effect of M2-like macrophages on HCC cell proliferation and invasion.

To identify the effect of IL-13 or IFN-α on Huh7 cells, Huh7 cells were cultured in macrophage-conditioned medium (MCM) with/without macrophages (THP1 cells) treated with IL-13, IFN-α, or their combination (Supplementary Figure 2A-C). We found that IL-13 alone had a promoting effect on tumor proliferation and invasion, but that this promoting effect was more robust in cells co-cultured with macrophages. By contrast, we did not observe a significant pro-tumor effect of IFN-α in Huh7 cells in vitro, due to the lower expression of IFN receptors (IFN-R) in Huh7 cells (Supplementary Figure 2D). We observed a significant difference between the Huh7+MCM (IL-13) group and the Huh7+MCM (IFN-α+IL13) group, suggesting that IFN-α inhibited HCC by reprogramming the polarization of TAMs from M2 to M1 phenotypes rather than via direct effects on HCC.

IFN-α relieves TAM-mediated immunosuppression and increases intratumoral $CD8^+$ T cell infiltration during sorafenib treatment

To investigate the mechanism of the synergetic anti-tumor effects of combined IFN-α/sorafenib treatment, we used FACS to examine the proportions of $CD4^+$ T cells, $CD8^+$ T cells, and TAMs ($F4/80^+/CD11b^+$) in orthotopic liver tumors (**Figure 5A**, Supplementary Figure 3A, 3B). In orthotopic Hepa1-6 tumors, we found that sorafenib alone induced a significant increase in TAM infiltration without any obvious changes in $CD4^+$ T and $CD8^+$ T cells, indicating a shift to an immunosuppressive status in the tumor

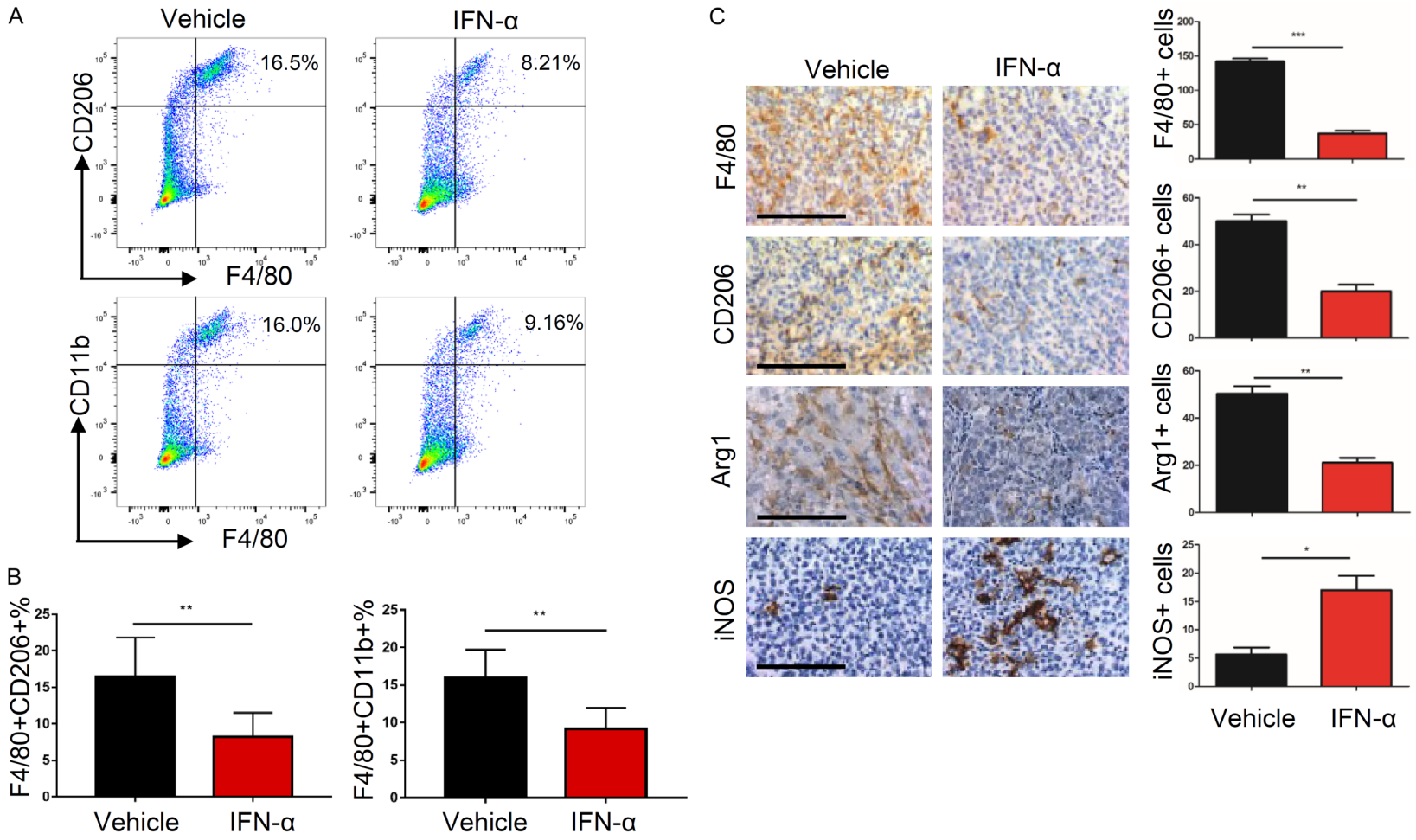

Figure 2. IFN-α inhibits tumor growth by altering tumor-associated macrophage polarization. (A, B) Representative flow cytometry plots (A) and quantification (B) showing the proportion of M2-like macrophages ($F4/80^+CD206^+$ and $F4/80^+CD11b^+$) in Hepa1-6 orthotopic tumor samples from C57BL/6 mice. (C) Representative immunohistochemistry images (left panels) and quantified data (right panels) of F4/80, CD206, Arg1, and iNOS in liver cancer tissues. Scale bar: 100 μm. Error bars indicate mean ± SEM. $*P < 0.05$ and $**P < 0.01$.

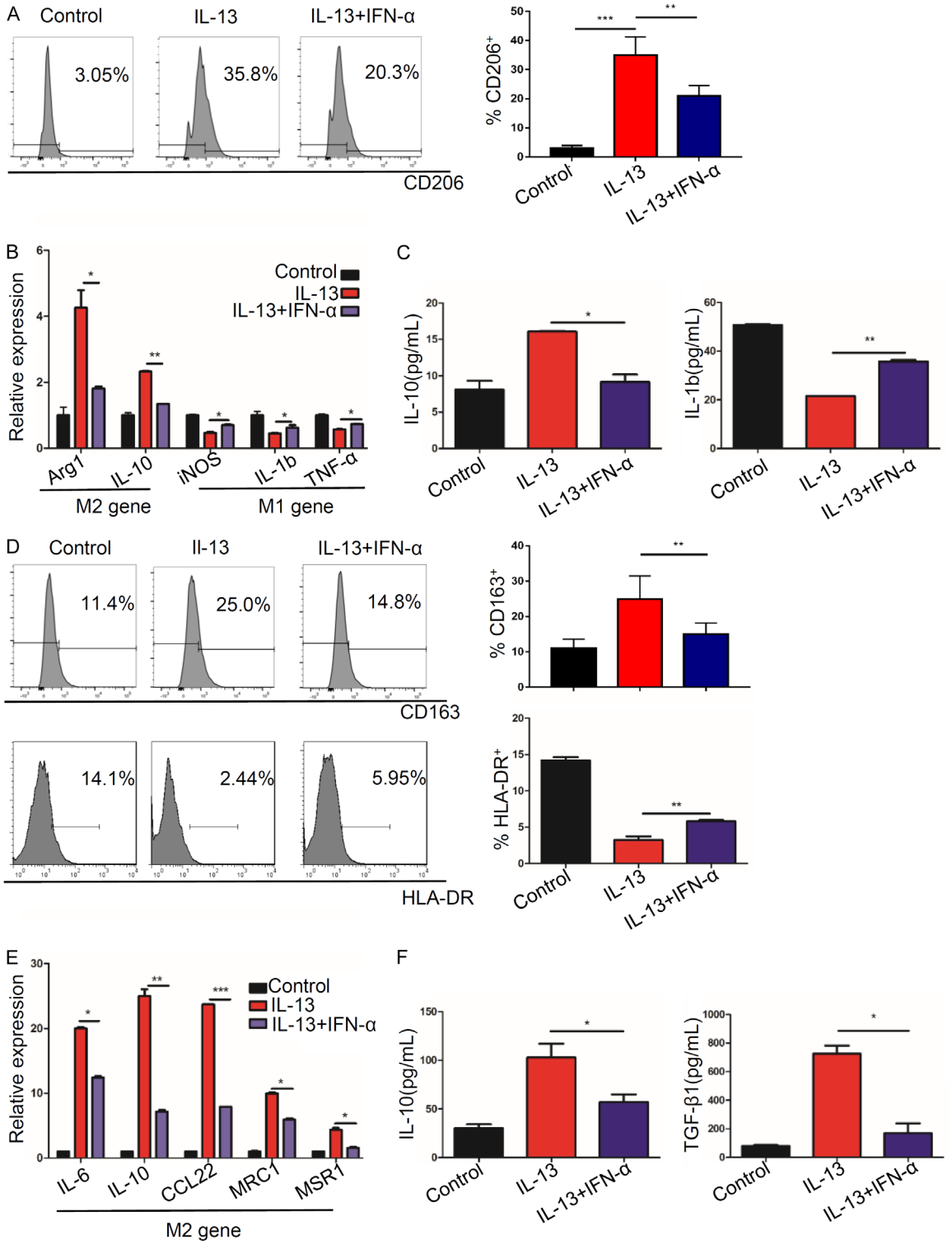

Figure 3. IFN-α inhibits M2-like polarization of TAMs induced by IL-13 *in vitro*. A. RAW264.7 cells were treated with IL-13 (20 ng/ml), IFN-α (10^4 U/mL), or the combination for 72 h. The expression level of the M2 marker CD206 was analyzed via FACS. B. qPCR analysis of the expression levels of M2 markers (Arg-1, IL-10) and M1 markers (iNOS, IL-1b and TNF-α). C. The supernatant IL-10 and IL-1b levels measured via ELISA. D. Human THP-1 cells were treated with IL-13 (20 ng/ml), IFN-α (10^4 U/mL), or the combination for 72 h. The expression level of the M2 marker CD163 and the M1 marker HLA-DR were analyzed via FACS. E. qPCR analysis of the expression levels of M2 markers (IL-6, IL-10, CCL22, MRC1, and MSR1). F. Supernatant IL-10 and TGF-β1 levels measured via ELISA. Error bars indicate mean ± SEM. **P* < 0.05, ***P* < 0.01 and ****P* < 0.001.

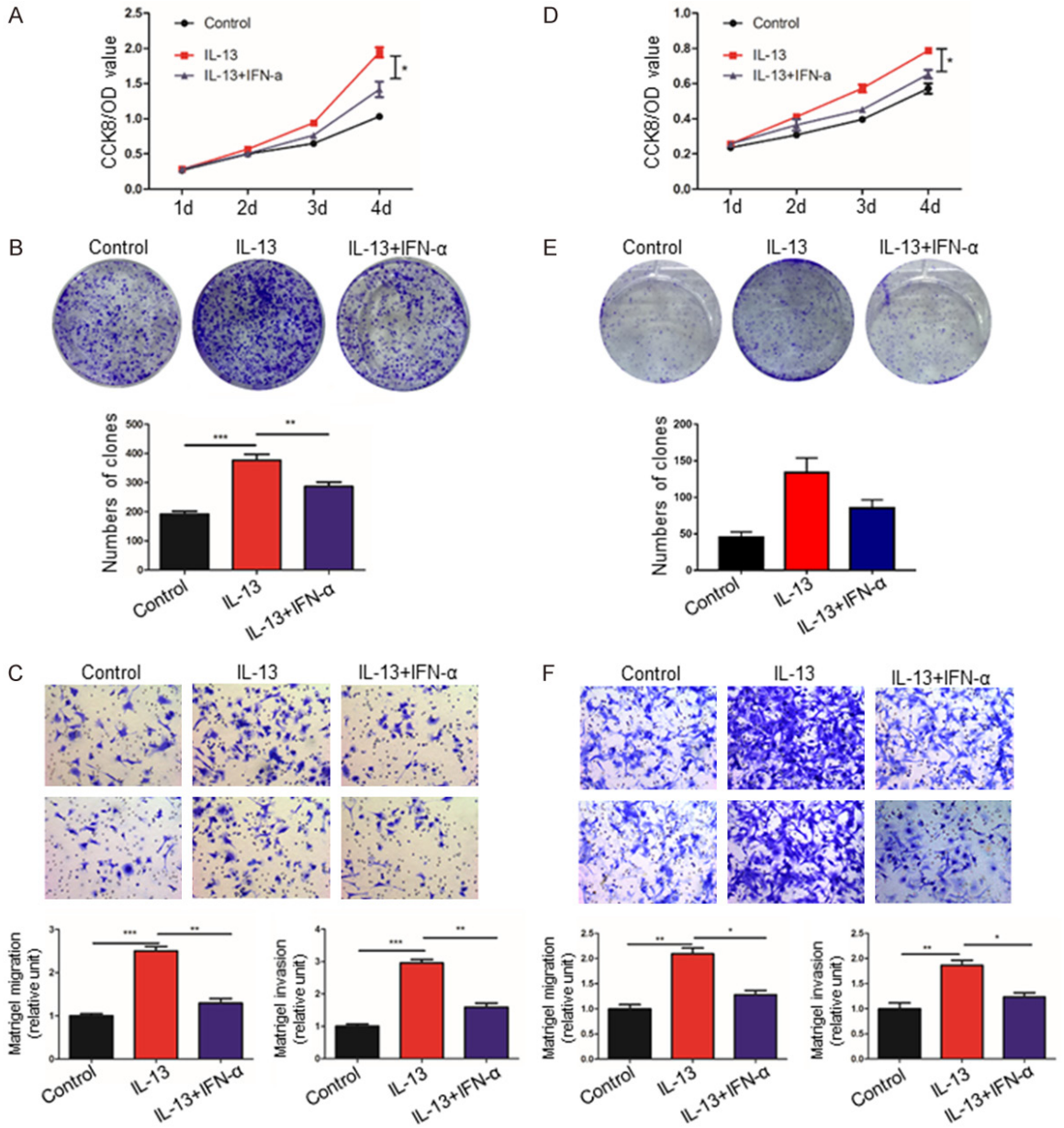

Figure 4. IFN-α eliminates TAM-promoted HCC proliferation and migration *in vitro*. RAW264.7 and THP-1 cells were treated with IL-13 (20 ng/ml), IFN-α (10^4 U/mL), or the combination for 72 h, and the culture medium was replaced with serum-free fresh medium. 24 h later, the supernatant was collected as macrophage-conditioned medium (MCM). A. Hepa1-6 cells were cultured in MCM for 96 h, and cell vitality was determined via Cell Counting Kit-8 assays. B. Hepa1-6 cells were cultured with MCM, and cell proliferation was assessed via colony-forming assays. C. The migration and invasive abilities of Hepa1-6 cells were evaluated via transwell assays 24 h post-treatment. D. Huh7 cells were cultured in MCM for 96 h, and cell vitality was determined via Cell Counting Kit-8 assays. E. Huh7 cells were cultured in CM, and cell proliferation was assessed via colony-forming assays. F. The effects of different MCMs on Huh7 migration and invasion were evaluated via transwell assays 24 h post-treatment.

microenvironment. IFN-α treatment significantly inhibited the M2-like polarization of TAMs and increased intratumoral infiltration by $CD4^+$ T cells and $CD8^+$ T cells. Moreover, treatment with a combination of sorafenib and IFN-α also resulted in a significant reduction in the proportion of TAMs and an increase in the proportion of $CD8^+$ T cells, indicating that sorafenib could induce neutralization of the immunosuppressive state in the tumor microenvironment (**Figure 5A**). Our IHC staining also revealed a decrease in the proportion of $F4/80^+$ TAMs and

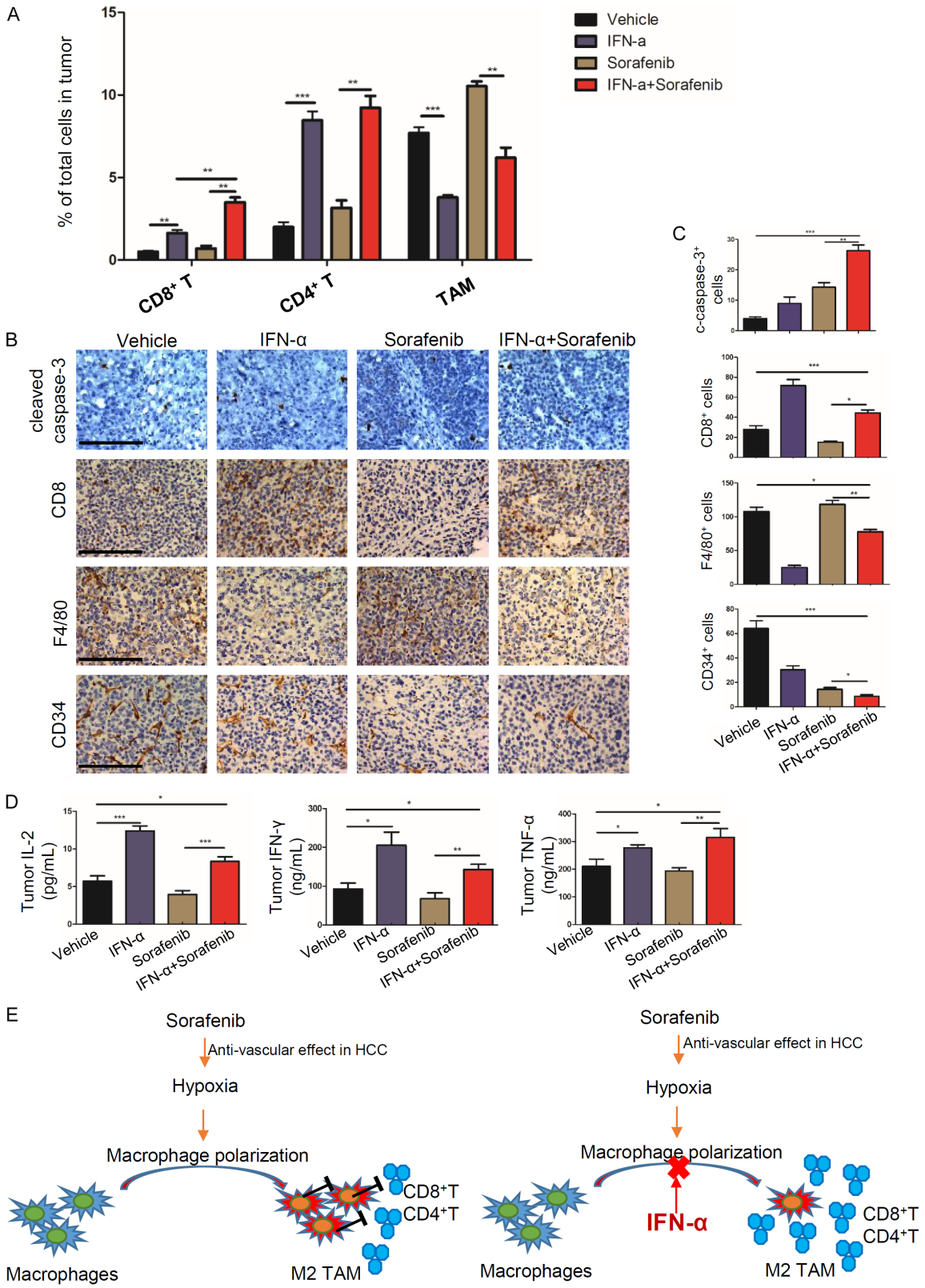

Figure 5. IFN-α relieves TAM-mediated immunosuppression and increases intratumoral CD8⁺ T cell infiltration during sorafenib treatment. (A) The proportions of intratumoral CD4⁺ T, CD8⁺ T cells, and TAMs (F4/80⁺/CD11b⁺) were quantified via FACS. (B, C) Representative immunohistochemistry (B) and quantification (C) of cleaved caspase-3, CD8, F4/80 and CD34 in tumors after treatment. Scale bar: 100 μm. (D) The supernatant levels of IL-2, IFN-γ and TNF-α were measured via ELISA. (E) A schematic description of the mechanisms involved in the sorafenib/IFN-α effects presented in this study. Error bars indicate mean ± SEM. **P* < 0.05, ***P* < 0.01 and ****P* < 0.001.

an increase in the proportion of $CD8^+$ T cells in Hepa1-6 tumors (**Figure 5B**, **5C**) after combined IFN-α/sorafenib treatment. Via ELISAs, we also evaluated the levels of proteins that serve as markers for activation of tumor-infiltrating $CD8^+$ T cells. We found that IFN-α in combination with sorafenib significantly increased the intratumoral levels of IL-2, IFN-γ, and TNF-α compared with their levels in the controls (**Figure 5D**). IHC staining demonstrated a significant increase in apoptosis (via cleaved caspase-3 and TUNEL staining) and a decrease in angiogenesis (CD34) in the IFN-α/sorafenib treatment group compared with the effects in the other groups (**Figure 5B**, **5C** and Supplementary Figure 4A, 4B).

Our combined findings suggest that IFN-α treatment can neutralize the immunosuppressive status in tumor microenvironments induced by the M2-like polarization of TAMs after sorafenib treatment and increase the proportion of $CD8^+$ T cells (**Figure 5E**).

Discussion

HCC is an aggressive cancer with a very poor prognosis [2]. The outlook for the mortality rate of liver cancer patients is still not optimistic in China [23], and it is also significantly increased in the United States [24]. Even though considerable progress has been made in HCC treatment over the past decades, the current challenges in its treatment are mainly driven by the tendency of patients to have advanced stage cancer and a high incidence of metastasis at the time of diagnosis as well as by a lack of effective treatments. Angiogenesis is considered a hallmark of cancer progression, and blocking the induction of angiogenesis can inhibit tumor growth and metastasis [25]. Sorafenib, the current first line treatment for advanced-stage HCC, is an angiogenesis inhibitor [26, 27]; however, therapeutic efficacy of sorafenib for HCC patients is still not satisfactory. Anti-angiogenic therapies that target VEGFR, including sorafenib, promote more invasive and metastatic behaviors in cancer cells [28, 29]; therefore, because sorafenib alone is not an effective treatment for HCC patients, it is critical to identify effective combination treatments.

Many studies have revealed that IFN-α has antiviral, immunomodulatory, and anti-proliferative effects on HCC as well as on other types of cancer [30-32]. Several clinical trials have demonstrated that HCC patients derive significant benefits from IFN-α treatment in terms of both overall and disease-free survival [18, 19]. IFN-α is often used as an adjunct therapy in the treatment of cancer patients, and its use in combination therapy has been extensively studied in the past decade. In particular, a recent study indicated that a combination of anti-CD20 Ab and IFN-α had a synergistic therapeutic effect in lymphoma treatment [33]. Furthermore, combined treatment with IFN-α and BRAF inhibitor enhanced the anti-proliferative and immunomodulatory effects of IFN-α on $BRAF^{V600E}$-mutant melanoma [34]. Patients with untreated metastatic renal cell carcinoma (mRCC) benefited from combined treatment with sorafenib and IFN-α [35]. Here we demonstrated that IFN-α enhances sorafenib's antitumor effect in HCC treatment. In *in vivo* mouse models, a combination of IFN-α had synergistic inhibitory effects on tumor growth and pulmonary metastasis of HCC without obvious toxicity.

TAMs, a major component of tumor immune microenvironments, are mainly polarized into an activated M2 phenotype [11, 20]. Many studies have shown that TAMs can modulate and shape HCC immune microenvironments and promote HCC growth, metastasis, and immune evasion [36-39]. The results of the current study showed that sorafenib treatment elevated TAM infiltration in HCC, resulting in an immunosuppressive HCC microenvironment. Interestingly, IFN-α could inhibit the polarization of macrophages into an M2-like phenotype, thereby neutralizing the promoting effects of M2-like macrophages on HCC cell proliferation and invasion. Moreover, IFN-α relieved TAM-mediated immunosuppression and increased intratumoral $CD8^+$ T cell infiltration by shifting macrophages towards the M1 phenotype during sorafenib treatment.

Via its antiangiogenic effects, sorafenib induces a reduction of microvascular density, which can promote intratumoral hypoxia [40]. Accumulating evidence shows that sorafenib induces intratumoral hypoxia, and cellular responses mediated by hypoxia-induced factors can favor selection of resistant cells adapted to the hypoxic microenvironment [41]. Our results demonstrated that sorafenib can induce the

macrophage polarization *in vivo* but not *in vitro*, and we speculate that this inconsistency is partly due to the hypoxic microenvironment induced by its antiangiogenic effects. Some evidence has shown that hypoxic conditions promote polarization of macrophages toward the M2 phenotype and modify inflammatory microenvironments by decreasing proinflammatory cytokine release [42]. Thus, we conclude that IFN-α can function as an immunomodulator that, when combined with sorafenib, results in increased therapeutic efficacy via a shift in TAM polarization and enhanced $CD8^+$ T cells infiltration, thus improving $CD8^+$ T cell activation in the HCC microenvironment.

In summary, we have demonstrated here that in HCC treatment, the synergistic anti-tumor effects of a combination of IFN-α and sorafenib are likely mediated by a transition from M2 to M1 macrophages induced by IFN-α. We propose that clinical use of IFN-α and sorafenib combination therapy holds promise for patients with advanced HCC.

Acknowledgements

This work was supported by the National Key Research and Development Program of China (2017YFC1308604); the Joint Tackling Project of Emerging Frontier Technologies in Shanghai Hospitals in 2017 (SHDC12017122); the National Key Basic Research Program of China (2014CB542101 and 2013CB910500); the National Natural Science Foundation of China (81772563, 81902390 and 81902952); and the Program of Shanghai Academic Research Leader (20XD1400900).

Disclosure of conflict of interest

None.

Address correspondence to: Lun-Xiu Qin and Qiong-Zhu Dong, Department of General Surgery, Huashan Hospital of Fudan University, Shanghai 200040, China; Cancer Metastasis Institute, Huashan Hospital of Fudan University, Shanghai 200040, China; Institutes of Biomedical Sciences, Fudan University, Shanghai 200040, China. Tel: +86-21-5288-7174; Fax: +86-21-5288-7174; E-mail: qinlx@fudan.edu.cn (LXQ); qzhdong@fudan.edu.cn (QZD); Hu-Liang Jia, Department of General Surgery, Huashan Hospital of Fudan University, Shanghai 200040, China; Cancer Metastasis Institute, Huashan Hospital of Fudan University, Shanghai 200040, China. Tel: +86-21-5288-7174; Fax: +86-21-5288-7174; E-mail: jbl-1@163.com

References

[1] Guerra F and Levi Sandri GB. The problem of the most appropriate curative treatment for hepatocellular carcinoma. When to embolize? When to operate? J Hepatol 2015; 63: 280-281.

[2] Torre LA, Bray F, Siegel RL, Ferlay J, Lortet-Tieulent J and Jemal A. Global cancer statistics, 2012. CA Cancer J Clin 2015; 65: 87-108.

[3] Keating GM. Sorafenib: a review in hepatocellular carcinoma. Target Oncol 2017; 12: 243-253.

[4] Harding JJ, El Dika I and Abou-Alfa GK. Immunotherapy in hepatocellular carcinoma: primed to make a difference? Cancer 2016; 122: 367-377.

[5] Zou W. Immunosuppressive networks in the tumour environment and their therapeutic relevance. Nat Rev Cancer 2005; 5: 263-274.

[6] Finn OJ. Cancer immunology. N Engl J Med 2008; 358: 2704-2715.

[7] Peng D, Kryczek I, Nagarsheth N, Zhao L, Wei S, Wang W, Sun Y, Zhao E, Vatan L, Szeliga W, Kotarski J, Tarkowski R, Dou Y, Cho K, Hensley-Alford S, Munkarah A, Liu R and Zou W. Epigenetic silencing of TH1-type chemokines shapes tumour immunity and immunotherapy. Nature 2015; 527: 249-253.

[8] Deng L, Liang H, Xu M, Yang X, Burnette B, Arina A, Li XD, Mauceri H, Beckett M, Darga T, Huang X, Gajewski TF, Chen ZJ, Fu YX and Weichselbaum RR. STING-dependent cytosolic DNA sensing promotes radiation-induced type i interferon-dependent antitumor immunity in immunogenic tumors. Immunity 2014; 41: 843-852.

[9] Killock D. Immunotherapy: nivolumab keeps HCC in check and opens avenues for checkmate. Nat Rev Clin Oncol 2017; 14: 392.

[10] Zhu D, Liu L, Yang D, Fu S, Bian Y, Sun Z, He J, Su L, Zhang L, Peng H and Fu YX. Clearing persistent extracellular antigen of hepatitis B virus: an immunomodulatory strategy to reverse tolerance for an effective therapeutic vaccination. J Immunol 2016; 196: 3079-3087.

[11] Noy R and Pollard JW. Tumor-associated macrophages: from mechanisms to therapy. Immunity 2014; 41: 49-61.

[12] Ao JY, Zhu XD, Chai ZT, Cai H, Zhang YY, Zhang KZ, Kong LQ, Zhang N, Ye BG, Ma DN and Sun HC. Colony-stimulating factor 1 receptor blockade inhibits tumor growth by altering the polarization of tumor-associated macrophages in hepatocellular carcinoma. Mol Cancer Ther 2017; 16: 1544-1554.

[13] Pyonteck SM, Akkari L, Schuhmacher AJ, Bowman RL, Sevenich L, Quail DF, Olson OC, Quick ML, Huse JT, Teijeiro V, Setty M, Leslie CS, Oei Y, Pedraza A, Zhang J, Brennan CW, Sutton JC, Holland EC, Daniel D and Joyce JA. CSF-1R inhibition alters macrophage polarization and blocks glioma progression. Nat Med 2013; 19: 1264-1272.

[14] Zhang W, Zhu XD, Sun HC, Xiong YQ, Zhuang PY, Xu HX, Kong LQ, Wang L, Wu WZ and Tang ZY. Depletion of tumor-associated macrophages enhances the effect of sorafenib in metastatic liver cancer models by antimetastatic and antiangiogenic effects. Clin Cancer Res 2010; 16: 3420-3430.

[15] Feldman DR, Kondagunta GV, Schwartz L, Patil S, Ishill N, DeLuca J, Russo P and Motzer RJ. Phase II trial of pegylated interferon-alpha 2b in patients with advanced renal cell carcinoma. Clin Genitourin Cancer 2008; 6: 25-30.

[16] Hansson J, Aamdal S, Bastholt L, Brandberg Y, Hernberg M, Nilsson B, Stierner U and von der Maase H; Nordic Melanoma Cooperative Group. Two different durations of adjuvant therapy with intermediate-dose interferon alfa-2b in patients with high-risk melanoma (Nordic IFN trial): a randomised phase 3 trial. Lancet Oncol 2011; 12: 144-152.

[17] Chen LT, Chen MF, Li LA, Lee PH, Jeng LB, Lin DY, Wu CC, Mok KT, Chen CL, Lee WC, Chau GY, Chen YS, Lui WY, Hsiao CF, Whang-Peng J and Chen PJ. Long-term results of a randomized, observation-controlled, phase III trial of adjuvant interferon Alfa-2b in hepatocellular carcinoma after curative resection. Ann Surg 2012; 255: 8-17.

[18] Sun HC, Tang ZY, Wang L, Qin LX, Ma ZC, Ye QH, Zhang BH, Qian YB, Wu ZQ, Fan J, Zhou XD, Zhou J, Qiu SJ and Shen YF. Postoperative interferon alpha treatment postponed recurrence and improved overall survival in patients after curative resection of HBV-related hepatocellular carcinoma: a randomized clinical trial. J Cancer Res Clin Oncol 2006; 132: 458-465.

[19] Lo CM, Liu CL, Chan SC, Lam CM, Poon RT, Ng IO, Fan ST and Wong J. A randomized, controlled trial of postoperative adjuvant interferon therapy after resection of hepatocellular carcinoma. Ann Surg 2007; 245: 831-842.

[20] Chanmee T, Ontong P, Konno K and Itano N. Tumor-associated macrophages as major players in the tumor microenvironment. Cancers (Basel) 2014; 6: 1670-1690.

[21] Furudate S, Fujimura T, Kakizaki A, Hidaka T, Asano M and Aiba S. Tumor-associated M2 macrophages in mycosis fungoides acquire immunomodulatory function by interferon alpha and interferon gamma. J Dermatol Sci 2016; 83: 182-189.

[22] Yang X, Zhang X, Fu ML, Weichselbaum RR, Gajewski TF, Guo Y and Fu YX. Targeting the tumor microenvironment with interferon-beta bridges innate and adaptive immune responses. Cancer Cell 2014; 25: 37-48.

[23] Chen W, Zheng R, Baade PD, Zhang S, Zeng H, Bray F, Jemal A, Yu XQ and He J. Cancer statistics in China, 2015. CA Cancer J Clin 2016; 66: 115-132.

[24] Llovet JM, Zucman-Rossi J, Pikarsky E, Sangro B, Schwartz M, Sherman M and Gores G. Hepatocellular carcinoma. Nat Rev Dis Primers 2016; 2: 16018.

[25] Hanahan D and Weinberg RA. Hallmarks of cancer: the next generation. Cell 2011; 144: 646-674.

[26] Llovet JM, Ricci S, Mazzaferro V, Hilgard P, Gane E, Blanc JF, de Oliveira AC, Santoro A, Raoul JL, Forner A, Schwartz M, Porta C, Zeuzem S, Bolondi L, Greten TF, Galle PR, Seitz JF, Borbath I, Haussinger D, Giannaris T, Shan M, Moscovici M, Voliotis D and Bruix J; KEYNOTE-224 investigators. Sorafenib in advanced hepatocellular carcinoma. N Engl J Med 2008; 359: 378-390.

[27] Cheng AL, Kang YK, Chen Z, Tsao CJ, Qin S, Kim JS, Luo R, Feng J, Ye S, Yang TS, Xu J, Sun Y, Liang H, Liu J, Wang J, Tak WY, Pan H, Burock K, Zou J, Voliotis D and Guan Z. Efficacy and safety of sorafenib in patients in the Asia-Pacific region with advanced hepatocellular carcinoma: a phase III randomised, double-blind, placebo-controlled trial. Lancet Oncol 2009; 10: 25-34.

[28] Ebos JM, Lee CR, Cruz-Munoz W, Bjarnason GA, Christensen JG and Kerbel RS. Accelerated metastasis after short-term treatment with a potent inhibitor of tumor angiogenesis. Cancer Cell 2009; 15: 232-239.

[29] Paez-Ribes M, Allen E, Hudock J, Takeda T, Okuyama H, Vinals F, Inoue M, Bergers G, Hanahan D and Casanovas O. Antiangiogenic therapy elicits malignant progression of tumors to increased local invasion and distant metastasis. Cancer Cell 2009; 15: 220-231.

[30] Clavien PA. Interferon: the magic bullet to prevent hepatocellular carcinoma recurrence after resection? Ann Surg 2007; 245: 843-845.

[31] Yang Y, Zhou Y, Hou J, Bai C, Li Z, Fan J, Ng IOL, Zhou W, Sun H, Dong Q, Lee JMF, Lo CM, Man K, Yang Y, Li N, Ding G, Yu Y and Cao X. Hepatic IFIT3 predicts interferon-alpha therapeutic response in patients of hepatocellular carcinoma. Hepatology 2017; 66: 152-166.

[32] Herrmann E, Brinkmann OA, Bode ME, Bierer S, Kopke T, Bogemann M, Hertle L and Wulfing C. Histologic subtype of metastatic renal cell carcinoma predicts response to combined immunochemotherapy with interleukin 2, inter-

feron alpha and 5-fluorouracil. Eur Urol 2007; 51: 1625-1631; discussion 1631-1622.
[33] Xuan C, Steward KK, Timmerman JM and Morrison SL. Targeted delivery of interferon-alpha via fusion to anti-CD20 results in potent antitumor activity against B-cell lymphoma. Blood 2010; 115: 2864-2871.
[34] Sabbatino F, Wang Y, Scognamiglio G, Favoino E, Feldman SA, Villani V, Flaherty KT, Nota S, Giannarelli D, Simeone E, Anniciello AM, Palmieri G, Pepe S, Botti G, Ascierto PA, Ferrone CR and Ferrone S. Antitumor activity of BRAF inhibitor and IFNalpha combination in BRAF-mutant melanoma. J Natl Cancer Inst 2016; 108: djv435.
[35] Eto M, Kawano Y, Hirao Y, Mita K, Arai Y, Tsukamoto T, Hashine K, Matsubara A, Fujioka T, Kimura G, Shinohara N, Tatsugami K, Hinotsu S and Naito S; Japan RCC Trialist Collaborative Group (JRTCG) investigators. Phase II clinical trial of sorafenib plus interferon-alpha treatment for patients with metastatic renal cell carcinoma in Japan. BMC Cancer 2015; 15: 667.
[36] Eggert T, Wolter K, Ji J, Ma C, Yevsa T, Klotz S, Medina-Echeverz J, Longerich T, Forgues M, Reisinger F, Heikenwalder M, Wang XW, Zender L and Greten TF. Distinct functions of senescence-associated immune responses in liver tumor surveillance and tumor progression. Cancer Cell 2016; 30: 533-547.
[37] Li X, Yao W, Yuan Y, Chen P, Li B, Li J, Chu R, Song H, Xie D, Jiang X and Wang H. Targeting of tumour-infiltrating macrophages via CCL2/CCR2 signalling as a therapeutic strategy against hepatocellular carcinoma. Gut 2017; 66: 157-167.
[38] Huang W, Chen Z, Zhang L, Tian D, Wang D, Fan D, Wu K and Xia L. Interleukin-8 induces expression of FOXC1 to promote transactivation of CXCR1 and CCL2 in hepatocellular carcinoma cell lines and formation of metastases in mice. Gastroenterology 2015; 149: 1053-1067, e1014.
[39] Zhu Y, Yang J, Xu D, Gao XM, Zhang Z, Hsu JL, Li CW, Lim SO, Sheng YY, Zhang Y, Li JH, Luo Q, Zheng Y, Zhao Y, Lu L, Jia HL, Hung MC, Dong QZ and Qin LX. Disruption of tumour-associated macrophage trafficking by the osteopontin-induced colony-stimulating factor-1 signalling sensitises hepatocellular carcinoma to anti-PD-L1 blockade. Gut 2019; 68: 1653-1666.
[40] Mendez-Blanco C, Fondevila F, Garcia-Palomo A, Gonzalez-Gallego J and Mauriz JL. Sorafenib resistance in hepatocarcinoma: role of hypoxia-inducible factors. Exp Mol Med 2018; 50: 1-9.
[41] Liang Y, Zheng T, Song R, Wang J, Yin D, Wang L, Liu H, Tian L, Fang X, Meng X, Jiang H, Liu J and Liu L. Hypoxia-mediated sorafenib resistance can be overcome by EF24 through Von Hippel-Lindau tumor suppressor-dependent HIF-1alpha inhibition in hepatocellular carcinoma. Hepatology 2013; 57: 1847-1857.
[42] Henze AT and Mazzone M. The impact of hypoxia on tumor-associated macrophages. J Clin Invest 2016; 126: 3672-3679.

Supplementary Table 1. Primer sequence of gene used for qPCR

Gene name	Primer sequence
Mouse	
Arg1	F: CTCCAAGCCAAAGTCCTTAGAG
Arg1	R: GGAGCTGTCATTAGGGACATCA
GAPDH	F: AGGTCGGAGTCAACGGATTTG
GAPDH	R: TGTAAACCATGTAGTTGAGGTCA
IL-10	F: GCTCTTGCACTACCAAAGCC
IL-10	R: CTGCTGATCCTCATGCCAGT
iNOS	F: GTTCTCAGCCCAACAATACAAGA
iNOS	R: GTGGACGGGTCGATGTCAC
IL-1b	F: GAAATGCCACCTTTTGACAGTG
IL-1b	R: TGGATGCTCTCATCAGGACAG
TNF-α	F: CAGGCGGTGCCTATGTCTC
TNF-α	R: CGATCACCCCGAAGTTCAGTAG
Human	
IL-6	F: ACTCACCTCTTCAGAACGAATTG
IL-6	R: CCATCTTTGGAAGGTTCAGGTTG
IL10	F: GGGAGCCCCTTTGATGATTAA
IL10	R: GCCACAGCTTTCAAGAATGAAGT
CCL22	F: ATCGCCTACAGACTGCACTC
CCL22	R: GACGGTAACGGACGTAATCAC
MRC1	F: TCCGGGTGCTGTTCTCCTA
MRC1	R: CCAGTCTGTTTTTGATGGCACT
MSR1	F: GCAGTGGGATCACTTTCACAA
MSR1	R: AGCTGTCATTGAGCGAGCATC
GAPDH	F: TGACTTCAACAGCGACACCCA
GAPDH	R: CACCCTGTTGCTGTAGCCAAA

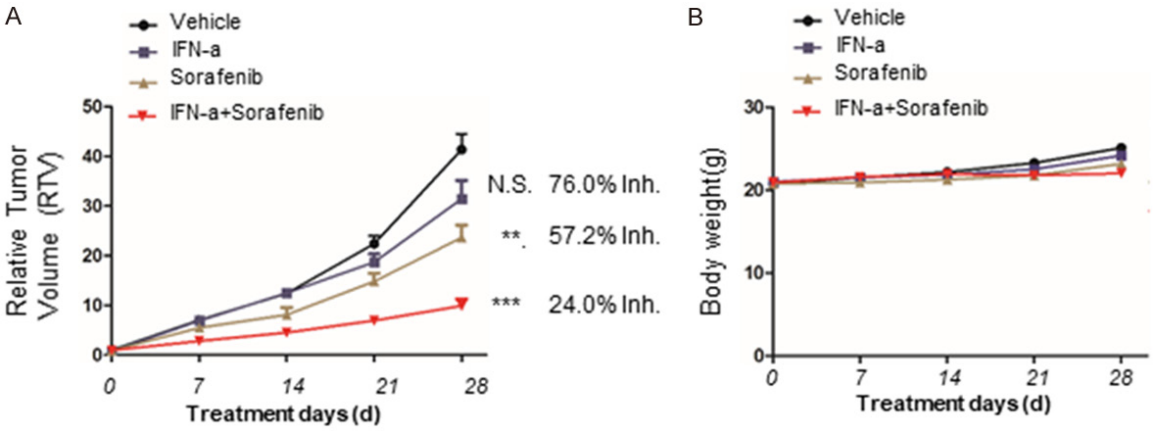

Supplementary Figure 1. IFN-α enhances the anti-tumor effect of sorafenib. A. The anti-tumor effect index of Hepa1-6 tumors with various treatments. B. Body weight changes of mice during with various treatments.

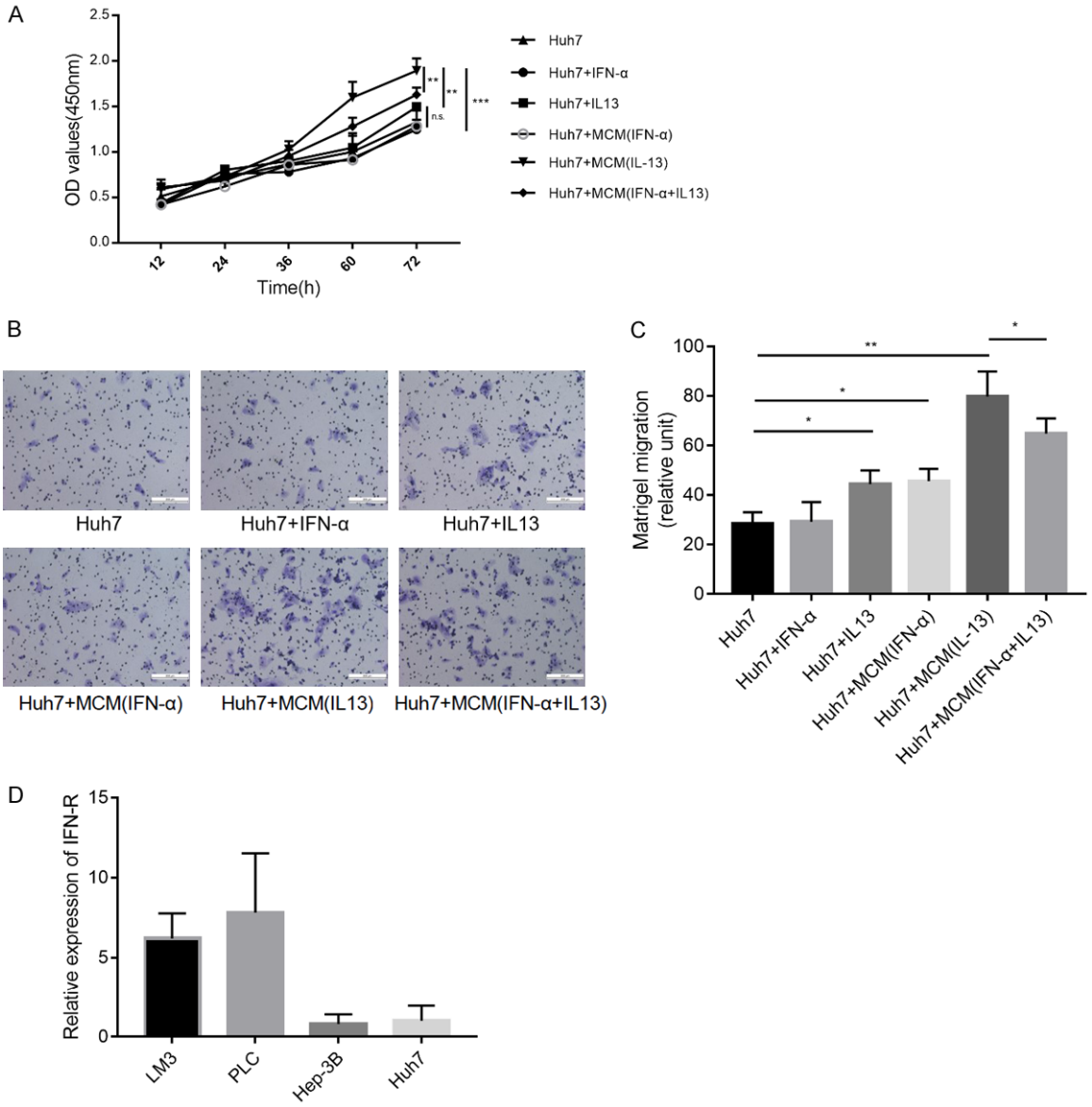

Supplementary Figure 2. THP-1 cells were treated with IL-13 (20 ng/ml), IFN-α (10^4 U/mL), or the combination for 72 h, and the culture medium was replaced with serum-free fresh medium. 24 h later, the supernatant was collected as macrophage-conditioned medium (MCM). A. 6 groups which are Huh7 (Huh7 cells alone), Huh7+IFN-α (Huh7 cells treated with IFN-α), Huh7+IL13 (Huh7 cells treated with IL13), Huh7+MCM (IFN-α) (Huh7 cells were cultured in MCM treated with IFN-α), Huh7+MCM (IL-13) (Huh7 cells were cultured in MCM treated with IL-13), Huh7+MCM (IFN-α+IL13) (Huh7 cells were cultured in MCM treated with IL-13 and IFN-α), cell vitality was determined via Cell Counting Kit-8 assays. B, C. The migration abilities of Huh7 cells were evaluated via transwell assays. D. Relative expression of IFN-α receptor (IFN-R) in HCC cell lines.

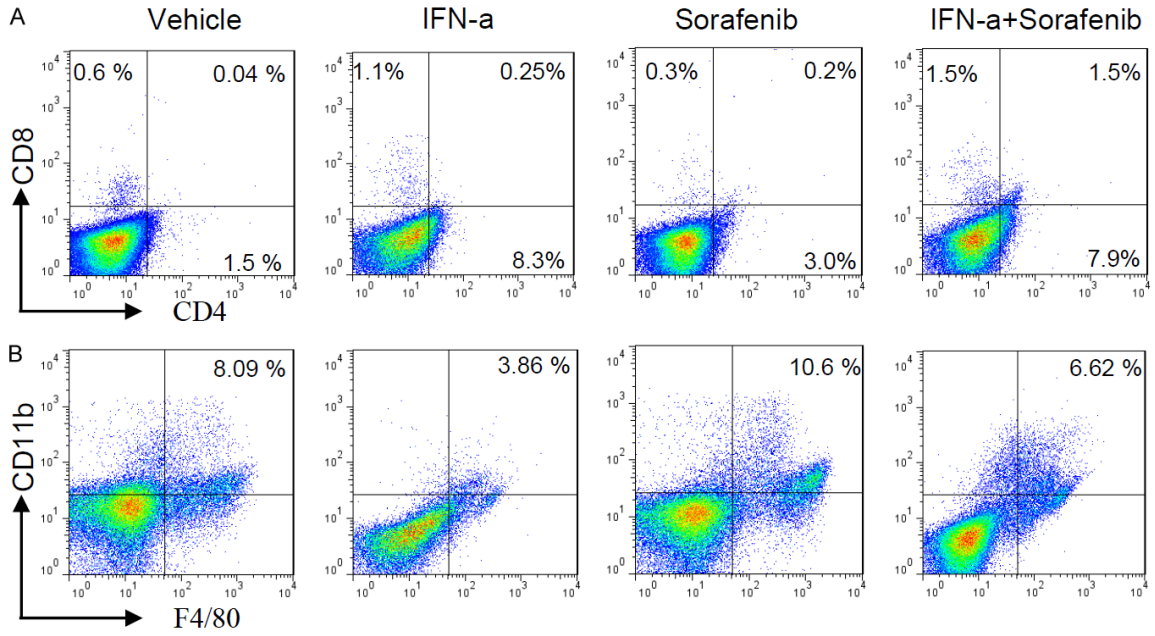

Supplementary Figure 3. Flow cytometry results showing the proportions of (A) T cells ($CD8^+$ T cells and $CD4^+$ T cells) and (B) TAM ($F4/80^+CD11b^+$) in Hepa1-6 orthotopic tumor tissues from C57BL/6 mice.

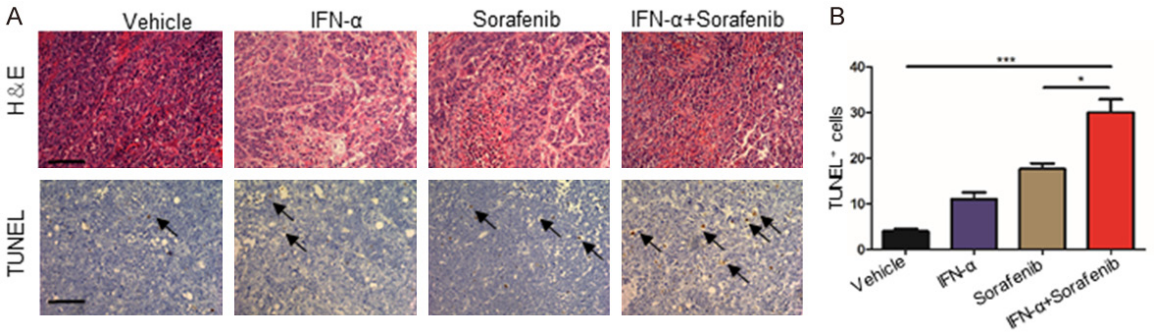

Supplementary Figure 4. IFN-α and sorafenib combination treatment enhanced HCC apoptosis. A. Representative immunohistochemical (IHC) images of Hematoxylin and Eosin (HE) and TUNEL in subcutaneous tumors treated as indicated. B. Quantitative data are shown as mean ± SEM and compared using Student's t-test.